THE UNIVERSITY OF MICHIGAN
COLLEGE OF ENGINEERING
Department of Chemical and Metallurgical Engineering

Final Report

SINTERING OF METAL OXIDES

G. Parravano

ORA Project 02832

under contract with:

SOLID STATE SCIENCES DIVISION
AIR FORCE OFFICE OF SCIENTIFIC RESEARCH
AIR RESEARCH AND DEVELOPMENT COMMAND
CONTRACT NO. AF 49(638)-493
PROJECT NO. 9762, TASK NO. 37621
WASHINGTON, D. C.

administered through:

OFFICE OF RESEARCH ADMINISTRATION ANN ARBOR

October 1963

TABLE OF CONTENTS

LIST OF ILLUSTRATIONS

I. OBJECTIVES

The research program, which was initiated in September 1958, had the following major objectives:

(a) To determine the transport mechanisms which control the sintering of a representative group of metal oxides;

(b) To relate the observed sintering mechanisms to fundamental properties of the solids (vapor pressure, diffusion coefficients, deviations from stoichiometric composition);

(c) To investigate the role of whisker growth in metal oxides on their sintering behavior;

(d) To assess the influence of surface effects on sintering in oxide compounds. At the time of termination of the contract, item (d) remained to be completed.

II. EXPERIMENTAL PROCEDURES

The experimental procedures and methods employed in carrying out the above studies include:

(a) Preparation of single crystal and polycrystalline microspheres of metal oxides (0.1 to 1 mm diameter) by means of special techniques and equipment;

(b) Observations on the rate of welding together of metal oxide microspheres with the aid of a hot stage permitting measurements under a variety of experimental conditions;

(c) Collection of information on the rate of growth of whiskers on metal oxide surfaces, by following whisker growth in sealed quartz vessels of special construction;

(d) X-ray, chemical and spectroscopic analysis of the crystals employed.

In addition, theoretical studies were carried out to derive mathematical expressions for the rate of sintering under conditions not covered by existing rate equations. The mathematical expression commonly used in sintering studies

is of the type:

$$\frac{x^n}{a^m} = kt \qquad (1)$$

where x, a, t are the diameter of the neck formed between sintered spheres, the diameter of the spheres and the time respectively. n, m, and k are constant at constant temperature. We have investigated the application of Eq. (1) to the growth of flat surfaces and bands on spherical surfaces and to sintering of spheres covered by such flat surfaces. In addition, theoretical expressions for the growth rate of whiskers under various transport mechanisms have been deduced.

III. EXPERIMENTAL RESULTS

A. SUMMARY

Some of the results obtained have been summarized in Technical Reports AFOSR TN 60-109, 60-1460, 59-184, and 59-481 and in publications listed in Section VI-C. The oxides investigated include ZnO, TiO_2, V_2O_5 and, in a qualitative fashion, NiO. The results on the sintering mechanism deduced from the experimental observations are summarized in Table I.

TABLE I

SUMMARY OF METAL OXIDES INVESTIGATED

Metal Oxide	Temp. Range (°C)	Sintering Mechanism	Driving Force	Remarks
ZnO	600-1050	Diffusion	Compositional gradient arising from physical or chemical conditions	Surface and bulk diffusion
	1050-1250	Distillation	Differences in vapor pressures	Controlling stages (a) evaporation rate; (b) diffusion through surface layer
V_2O_5	560-650	Diffusion	Compositional gradient	Initial welding provided by whisker growth
TiO_2	900-1350	Diffusion	Compositional gradient	Rate of welding influenced by facet formation

Whisker growth has been studied quantatively in the case of V_2O_5, but qualitative observations have been recorded for ZnO, TiO_2, and NiO. The formation of flat facets and surface bands has been studied on TiO_2.

In the subsequent sections we shall review the salient results for each oxide listed in Table I. For studies which have already been published only a brief mention of the conclusions will be given.

B. ZINC OXIDE

At temperatures below ≈900°C, sintering of nonstoichiometric zinc oxide was found to be controlled by the equilibration reaction between the solid and the gas phase:[1]

$$Zn_{(i)} + \frac{1}{2} O_2(g) \rightarrow Zn^{+2}_{(\ell)} + O^{-2}(\ell) \qquad (2)$$

where $Zn_{(i)}$, $Zn_{(\ell)}$ correspond to interstitial and lattice zinc ions.

The expression giving the rate of sintering was derived as:

$$-\ell n \left[1 - \left(\frac{x}{x_m}\right)^2\right] = D \left(\frac{\pi}{a}\right)^2 t + \ell n \frac{\pi^2}{8} \qquad (3)$$

where x_m, D are the value of x for $t = \infty$, diffusion coefficient, respectively. This mechanism was supported by the values of the diffusion coefficient of $Zn_{(i)}$, $D = 1 \times 10^{-7}$ cm^2 sec^{-1} at 900°C and that of the activation energy $E_D = 18.0$ kcal $mole^{-1}$, computed from sintering runs. Both of these values are in agreement with literature values of the same quantities.

At temperatures between 900 and 1050°C it was found that physical sintering through bulk diffusion was predominant. However, above 1050°C the diffusional transport responsible for sintering was greatly overshadowed by the transfer of matter through the gas phase. The detailed results are reported elsewhere.[2] Three cases are possible: The transport through the gas phase may not be slowed down by convective phenomena. The rate of transfer is then controlled by the rate of evaporation and is independent of total pressure and gaseous flow rate, and it involves a rather high activation energy (109 kcal $mole^{-1}$). This mechanism tends to occur at total pressures of less than 1 atm. At higher pressures, diffusive control of the rate of evaporation may set in. Sintering becomes dependent on the total pressure (natural convection) and, at high flow velocities, should be proportional to a fractional power of the flow velocity of the carrier gas (forced convection). The energy values involved in solid diffusion and evaporation are the factors which determine the type of sintering to be followed.

It was possible to calculate from the sintering runs a value for the rate of evaporation in good agreement with published values. It was also found that the rate of welding of ZnO at high temperature tended to decrease with increasing air pressure around the sample, indicating that diffusional limitations to the evaporating flux could be present. The latter was traced to natural convection through a density gradient in the vapor of ZnO adjacent to the solid surface. This was confirmed by the calculation of the vapor pressure of ZnO by means of the experimental results using a model involving explicitly the thickness of the surface layer.

C. VANADIUM PENTOXIDE

The sintering of vanadium pentoxide microspheres was studied in the temperature range 560 to 650°C in air, with spheres of diameters varying from 0.2 to 0.9 mm. The experiments have shown that Eq. (1) is of the form $(x^4/a^2) = kt$. Since the composition of the surrounding atmosphere during the experiments (air) was similar to the composition of the atmosphere prevailing during the preparation of the vanadium pentoxide microspheres, it was assumed that the chemical composition of the oxide did not vary significantly in the course of sintering. In this case, therefore, no major contribution to sintering from a chemical reaction was to be expected. The report relationship between x and t time had been interpreted in the sense that sintering of vanadium pentoxide is controlled by a diffusional process, involving migration of vacancies along the surface and grain boundaries, which act as vacancy sink.[3] In view of the polycrystalline nature of the vanadium pentoxide used, grain processes were likely to be kinetically pronounced. The effect of temperature on the rate of sintering has been obtained by noting the time required to obtain a constant value of x at different temperatures. From these data, a value of 32 ±5 kcal mole^{-1} was calculated for the activation energy of sintering of vanadium pentoxide. The relatively low value of the activation energy supports the view of diffusion along grain boundaries.

D. SINTERING OF RUTILE

In the temperature range 900 to 1350°C, rutile microspheres were found to sinter according to a relationship of the type:

$$\frac{x^2}{a} = kt.^4$$

Particular attention was directed toward examining the initial period of sintering, with the intent of bringing to light the effect on the sintering rate of flat surfaces, which were found to appear on the spherical surface in the neck region during sintering.

The significant results of the experiments on TiO_2 were:

(1) The value of n in Eq. (1) is dependent upon the extent of sintering: initially, $n \approx 7$, while for later stages $n \approx 2$.

(2) The change from one value to the other occurs over a narrow range of the ratio $x/a \approx 0.075$.

(3) The values of the activation energy for sintering are similar for the two stages.

(4) No change of center-to-center distance between the sintering spheres could be detected.

(5) The exponent of m in Eq. (1) is 3.

(6) Reduced oxygen pressure increased sintering rate.

The rate expressions which have been derived for the growth of the contact area between particles are based on a spherical model.[5] Whenever flat regions develop in the neck area, this model becomes invalid, since the presence of facets introduces a different neck geometry. Therefore two different situations should be recognized in the neck region during the sintering of TiO_2 microspheres: (1) without the presence of facets, and (2) with the presence of flat surfaces.

Initially, the former situation occurs, but as sintering progresses and facets appear on the surface of the microspheres, the latter case should be considered. It is suggested that the sharp, consistent change in the value of n with time is the result of the change in the geometry of the neck area rather than a change in the physical mechanism. In addition, the strong temperature dependence of the time at which the change occurs, t_c, is consistent with the assumption that the length of this time is connected with a solid state rearrangement of the type involved in facet formation. Since the change in rate expression always occurs at similar amounts of sintering, it would seem that the transport mechanism responsible for sintering in the initial period is also responsible for the rearrangement required to produce the facets.

For $t < t_c$, sintering occurs between rutile microspheres which still retain their spherical characteristics in the neck region. The experimental results show that the value of the rate exponent n is ≈ 7. According to previous derivation,[5] this fact would indicate that transport by surface diffusion was prevalent. The corresponding rate expression is:

$$\left(\frac{x}{a}\right)^7 = \frac{16}{7} \frac{D_s \gamma \Omega^2 n_s}{a^4 kT} \qquad (4)$$

Taking a = 0.05 cm, γ (surface tension) = 10^3 ergs/cm^2, Ω (atomic volume) = 10^{-23} cm^3/atom, n_s (surface atom concentration) = 10^{14} atom/cm^2, and using the experimental results for x/a = 0.08 at t = 600 sec and T = 1100°C, a value for the surface diffusion coefficient D_s = 1.2 cm^2/sec can be calculated for sintering in reducing atmosphere. For a similar amount of sintering in air at the same temperature, it was found that $D_s = 3.0 \times 10^{-2}$ cm^2/sec. These values are much higher than expected.

These results, together with the observation that no change in the center-to-center distance was detected during sintering, would indicate that surface diffusion is a predominant mechanism of mass transport. The operation of a diffusion mechanism is strengthened by the large effect of the atmosphere on the rate of neck growth. For $t > t_c$, sintering occurs between rutile microspheres which have developed flat facets. The experimental results show that the rate exponent has a value $n \approx 2$. A previous derivation attributed this value to mass transport by a plastic or viscous flow mechanism.[4] However, rutile is a crystalline solid and the stresses which surface tension might develop in the neck region would probably not be sufficient to cause configurational changes in the system. Hence the plastic flow mechanism cannot be a large contributing factor in rutile for the conditions studied.

The activation energies for this second period are similar to those derived for the first period (≈70 kcal, mole^{-1}). Several rate expressions for the sintering of rutile spheres after the development of facets assuming various types of facet movements by parallel or rotational displacement have been investigated theoretically. Transport mechanisms involving volume and surface diffusion were considered, but no expression was found which could accommodate the n = 2 rate exponent, the m = 3 scaling factor, and the lack of shrinkage.[7] An empirical expression for the rate of contact area growth after facet formation has the form

$$\left(\frac{x}{a}\right) = \frac{kD\Omega\gamma t}{a^3 kT} \quad . \qquad (5)$$

Assuming a k value of 100, volume-diffusion coefficients can be calculated from the data at 1100°C to be $D_V = 4 \times 10^{-4}$ cm^2/sec for air and $D_V = 1.7 \times 10^{-4}$ cm^2/sec in reducing atmosphere. These coefficients are considerably higher than those calculated from the literature or those calculated for the initial period, assuming diffusion through the volume of the crystal.

IV. THEORETICAL STUDIES

We have examined theoretically the following problems in the area of the sintering behavior of solids:

(a) Changes in configuration in solids as they proceed toward the equilibrium shape and size;

(b) Sintering by migration of surface steps;

(c) Derivation of the rate of whisker growth under diffusional transport.

A. CHANGES IN CONFIGURATION OF SOLIDS BY DIFFUSIONAL MECHANISMS

In connection with the problem of understanding the formation of facets and the sintering in the presence of facets in TiO_2, it has been deemed important to investigate theoretically some diffusional mechanisms responsible for change in configuration of solids. From a kinetic standpoint, we may classify the overall transport of matter between two locations in a solid body as the sequence of three elementary steps. They are:

(1) The tearing down of atoms or building up of vacancies at the source of the transport;

(2) The transfer of atoms and vacancies in opposing directions between source and sink;

(3) The building up of atoms and tearing down of vacancies at the sink.

Atoms and vacancies are considered the carriers of mass. Kinetically, different rate expressions are obtained depending upon the relative rates of steps (1), (2), and (3). Whenever (1) and/or (3) are the slow steps of the sequence, the transport rate is controlled by the rate of carrier formation and destruction (nucleation, adsorption, decomposition). In all the subsequent derivations, we shall assume that processes (1) and (3) occur very fast so as to be considered equilibrium reactions.

We shall be concerned with mechanisms of mass transport controlled by surface and volume diffusion. The chemical potential difference needed for the establishment of the diffusional flux is taken to depend upon variations in the radius of curvature of the surface only, and any motivation resulting from concentration variations is disregarded. The discussion will cover the case where the chemical potentials of the carriers at the source and sink are constant. The derivation of the values of the chemical potentials at these locations has already been given[6] and we shall follow this derivation very

closely. Three possibilities exist for these calculations.

If surface-volume equilibrium is established, the chemical potentials are derived by writing down the variations in the surface free energy, δF_s, and bulk free energy, δF_v, for subracting or adding a differential amount of carriers, δN. In general, surface-volume equilibrium will be extablished whenever surface-volume migration is rapid enough, so that the free energy changes resulting from additions or subtractions of atoms from the surface are nearly numerically equal. This is a situation which obtains at high temperature, generally at $T > 0.5\ T_m$, where T_m is the melting point of the solid in °K. At lower temperatures, the surface-volume equilibrium is not established and the computation of the chemical potential difference is formally made in a similar fashion except that the free energy changes $\delta F'_s$ are related to the values $\delta F'_s$ corresponding to a layer of atoms directly above the surface (surface-surface equilibrium) or to δF_g which occurs in the gas phase (surface-gas equilibrium). We shall show, subsequently, that the boundary values of the chemical potentials which were obtained in all three cases are similar, so that in the following derivation we shall be concerned with the case of surface-volume equilibrium only.

1. Formation of Flat Facets on Curved Surfaces

Consider a circular facet which forms on a spherical surface by removal of material from the top of the facet or the addition of material around the perimeter of the facet. The occurrence of the first or the second type of growth is controlled by the relative values of γ_s and γ_F. In Fig. 1 we have depicted the former situation but the kinetic derivation of the growth process is similar for both cases. Let us assume that the facet grows by parallel displacement of itself as a result of the removal of material from its surface. Two paths are available to the carriers. Whenever surface diffusion is predominant the relationship between the facet diameter, x, and time can be derived following the method outlined in Ref. 6. The resulting equation is

$$x^5 = Kt \tag{6}$$

where

$$K = 4r^2\Omega^2 \frac{D_s n}{kT} (\gamma_s - \gamma_F).$$

If, however, conditions are such that volume diffusion predominates, the resulting rate expression has the form

$$x^4 = Kt \qquad (7)$$

where

$$K = 2r \frac{D_v \Omega}{kTk_1} .$$

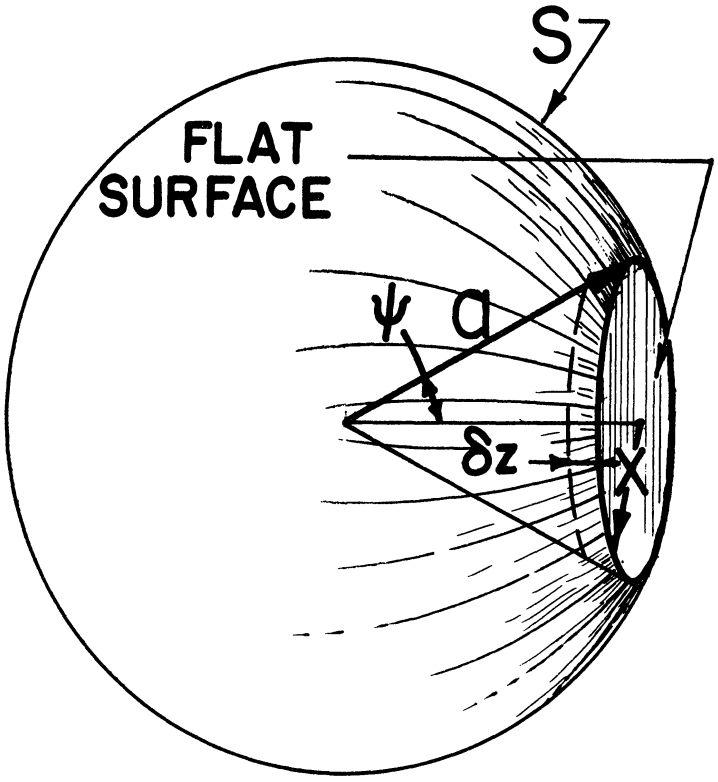

Fig. 1. Growth of circular facet on a spherical surface by removal of material from top of facet.

2. Contact Between Two Spheres by Parallel Displacement of Facets

Let us consider the growth of a connecting bridge between two spheres upon which facets have been formed and let us assume that the process occurs by parallel displacement of facets in the neck area. Consider facets growing outward after a time t_1 (time for facet formation). During this time, the contact will grow between the curved surfaces. We shall consider the case where both growths between curved and flat surfaces are controlled by the same mechanism. The geometrical model is shown in Fig. 2. The source of vacancies is the sphere surface and the sink is the facet in the neck region. Assume the neck intercepts the facets along the entire perimeter at the same time and that each facet meets the neck radius at the same angle. If the assumption of local surface-volume equilibrium holds, the relationship between surface and volume

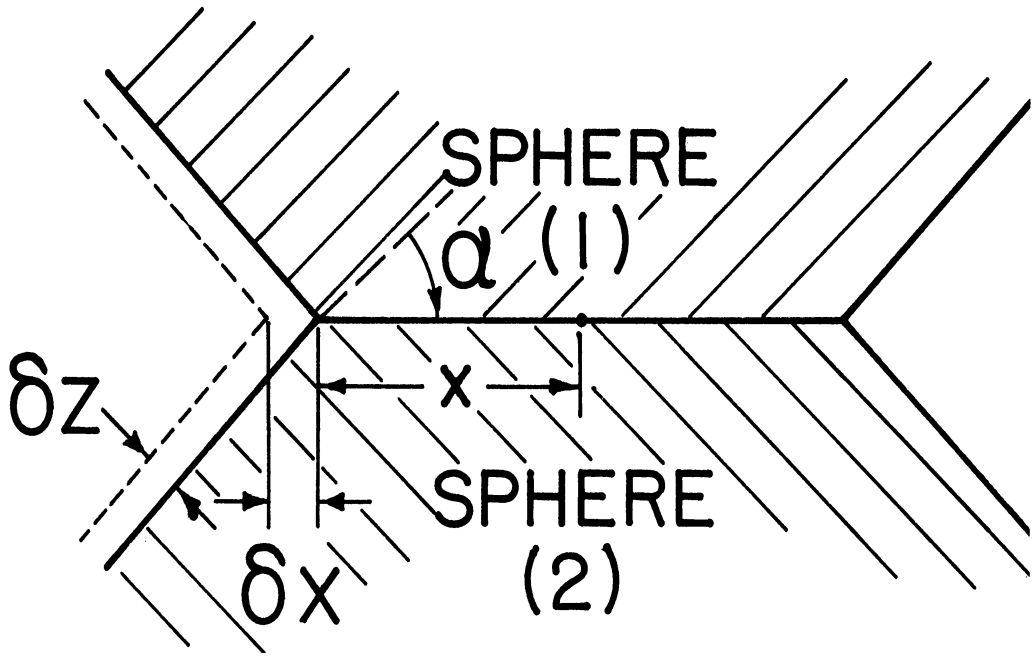

Fig. 2. Contact between spherical surfaces by parallel displacement of facets.

free energy may be calculated in a manner similar to the one used previously for the growth of a single facet. The results for different geometrical situations are summarized in Table II.

Facets may also grow by a rotational displacement around two fulcra situated along the boundary between the flat and the curved portion of the spheres (Fig. 3). The contact angle is not constant and the derived rate expressions for this situation are summarized in Table III.

TABLE II

GROWTH OF CONTACT BETWEEN SOLID SPHERES BY PARALLEL DISPLACEMENT OF FLAT SURFACES—SUMMARY OF RESULTS

Model	Parallel Facet Growth	Parallel Facet Growth	Interpenetration	
Vacancy source	Facet surface	Facet surface	Grain interior	Surface
Sink	Sphere surface	Sphere surface	Grain boundary	Grain boundary
Mechanism	Surface diffusion	Surface diffusion	Bulk diffusion	G. E. diffusion
dV/dt	$\pi \ell \cos\alpha(2x+\ell \sin\alpha)\delta x$	$2\pi \ell x \cos\alpha dx$	$\pi x^3 \frac{dx}{dt}$	$\pi x^3 \frac{dx}{dt}$
Perimeter	Constant $\propto R$	Constant $\propto R$	---	$2\pi x$
Area	---	---	πx^2	---
$\Delta(\mu-\mu_h)$	$-\frac{\Omega 4\pi x\gamma \sin\alpha}{\delta V}$	$-\frac{\pi 4\Omega x\gamma \sin\alpha}{\delta V}$	$\frac{2\gamma\Omega R}{x^2}$	$\frac{2\gamma\Omega R}{x^2}$
Path	ℓ	Constant $\propto R$	Constant $\propto R$	$\propto x$
Rate expression	$A \log x - Bx = kT$	$\frac{x^2}{kT\ell^3} = \frac{D_S n_S \Omega^2 \gamma}{\cos^2\alpha} \sin\alpha R$	$\frac{x^4}{R^4} = \frac{\gamma D_V \Omega \gamma t}{kTcR^3}$	$\left(\frac{x}{R}\right)^6 = \frac{24 D_S u_S \Omega^2}{kT} \frac{\gamma t}{cR^4}$
Scaling law	4	4	4	4

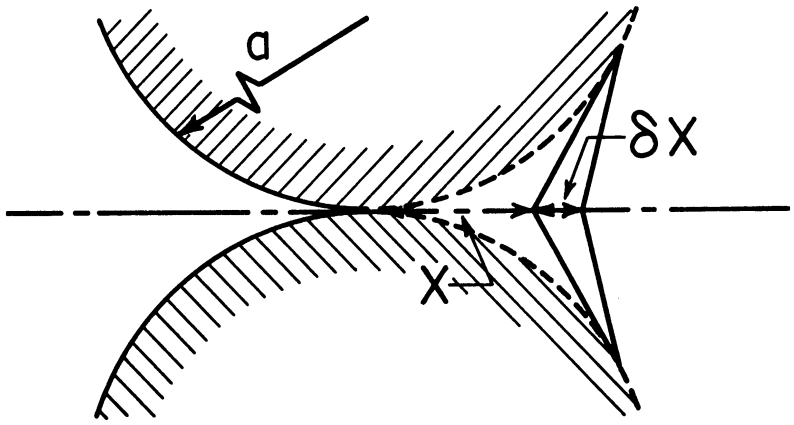

Fig. 3. Contact between spherical surfaces by rotational displacement of facets.

TABLE III

GROWTH OF CONTACT BETWEEN SOLID SPHERES BY ROTATIONAL DISPLACEMENT OF FACETS—SUMMARY OF RESULTS

Model	Fulcrum	Fulcrum
Vacancy source	Neck surface	---
Sink	Surface	---
Mechanism	Bulk diffusion	Surface diffusion
dV/dt	$\frac{4\pi x^3}{R}\frac{dx}{dt}$	$\frac{4\pi x^3}{R}\frac{dx}{dt}$
Perimeter	---	$4\pi x$
Area	$3\pi x^2$	---
$\Delta(\mu-\mu_h)$	$\frac{2\gamma R\Omega}{3x^2}$	$\frac{2\gamma R\Omega}{3x^2}$
Path	$\propto R$	Constant $\propto R$
Rate expression	$\left(\frac{x}{R}\right)^4 = \frac{2D\gamma t}{kTR^3}$	$\left(\frac{x}{R}\right)^5 = \frac{8D_n\Omega^2\gamma t}{kTR^4}$

3. Facet Formation on Curved Surface

Considering the situation involving surface diffusion and following the method outlined in Ref. 1, the variation in free energy following the transfer of ∂N carriers between a surface position on the sphere, s, and the flat plane, F, is given by $[(\mu-\mu_h)_s-(\mu-\mu_h)_F].dN$, where μ, μ_h are the chemical potentials of atoms and vacancies, respectively. The flux of migrating atoms will be a function of this potential and the path length. Since most faces of even cubic crystals show preferred directions for surface diffusion, the flux is given by.

$$j_\alpha = - \frac{\nu}{kT} \Sigma_\beta \Delta_{a\beta} \frac{\partial(\mu-\mu_h)}{\partial \zeta_\beta} \tag{8}$$

where

j flux of surface atoms (atoms/length-time)

$a\beta$ values for direction in surface plane

ζ coordinate of directions

ν number of surface atoms/area

With the above simplifying assumptions, Eq. (8) reduces to:

$$j = - \frac{D_s n_s}{kT} \nabla(\mu-\mu_h) \tag{9}$$

Let us assume that surface diffusion is anisotropic and the facet under consideration has a circular perimeter, P. This is the most reasonable assumption for an isotropic crystal. Then, it can be shown (Fig. 1) that

$$\delta F_s = (\gamma_F \cot \theta - \gamma_s \operatorname{cosec} \theta) \; 2\pi \sin \psi \delta z \tag{10}$$

$$\delta F_v = \left(\frac{\bar{\mu}-\bar{\mu}_h-\bar{\mu}_o}{} \right) A\delta z \tag{11}$$

Since the equilibrium condition is

$$\delta F_s + \delta F_v = 0$$

$$\left(\frac{\mu-\mu_h-\mu_o}{\Omega}\right) = -\frac{2\pi r \sin\psi}{A}(\gamma_F \cot\theta + \gamma_s \operatorname{cosc}\theta) \tag{12}$$

Taking a constant gradient across the flat facet and equal to

$$\nabla(\mu-\mu_h) = \frac{\bar{\mu}-\bar{\mu}_h-\bar{\mu}_o}{r} \tag{13}$$

where the bar indicates average values, and since

$$\frac{dV}{dt} = J\Omega\ell \tag{14}$$

where ℓ is the circumference of facet, and

$$dV = Adz \tag{15}$$

and substituting Eqs. (13)-(15) into (12)

$$\frac{Adz}{dt} = -\frac{2\pi r \sin\psi}{A}[\gamma_F \cot\theta - \gamma_s \operatorname{cosc}\theta]\frac{D_s n_s}{kT}\Omega^2\ell \tag{16}$$

Taking the characteristic facet dimension as its radius $x = r \sin\psi$ and for $\psi \ll \pi/2$:

$$\frac{d\psi}{dt} = \frac{1}{r}\frac{dx}{dt}.$$

Since $x^2 \ll r$, $A = \pi x^2$ and

$$z = (r^2-x^2)^{1/2} \quad \frac{dz}{dt} = \frac{1}{z}(-2x)\left(\frac{1}{r^2-x^2}\right)^{1/2}\frac{dx}{dt}$$

Substituting into Eq. (16) yields

$$\frac{x}{r}\frac{dx}{dt} = -\frac{2\pi x}{(\pi x^2)^2}\left[\gamma_F \cot\theta - \gamma_s \sec\theta\right]\frac{D_s n_s}{kT}\Omega^2 2\pi x$$

$$\frac{dx}{dt} = -\frac{4\pi r\Omega^2}{\pi x^3}\frac{D_s n_s}{kT}\left[\gamma_F \cot\theta - \gamma_s \sec\theta\right]$$

$$x^3\,dx = 4\pi\Omega^2\frac{D_s n_s}{kT}\left[\gamma_s \csc\theta - \gamma_F \cot\theta\right]dt$$

But $\csc\theta \cong \cot\theta$ for $\pi/12$

$$\csc\theta = \pi/x$$

and finally,

$$x^5 = 4r^2\Omega^2\frac{D_s n_s}{kT}(\gamma_s - \gamma_F)\,t$$

Whenever volume diffusion predominates, the rate equation becomes:

$$\frac{dV}{dt} = J\Omega A \qquad (17)$$

Upon substitution of Eqs. (9) and (15) into (17) the result is:

$$x^4 = 2r\frac{D_v\Omega}{kTk_1}\,t$$

B. SINTERING BY MIGRATION OF SURFACE STEPS

The decrease in surface energy, which is the motivation for physical sintering, can also be thought to occur by means of migration of surface steps. Let $C(r,t)$ be the surface concentration of a species which is part of the surface. $C(r,t)$ differs from the equilibrium composition. The equation expressing the flow of step under these conditions using spherical geometry is:

$$\frac{1}{\sin\theta}\frac{\partial}{\partial\theta}\left(\sin\theta\frac{\partial C}{\partial\theta}\right) = \frac{a^2}{D}\frac{\partial C}{\partial t} \qquad (18)$$

where D, $\bar{a}$ are the diffusion constant and the average radius of the spherical particle before and after sintering.

By solving Eq. (18) the following rate law for the neck growth was obtained:

$$\left(\frac{x}{\bar{a}}\right)^2 \simeq \left(\frac{8}{7}\right)\frac{C_o}{\rho}\frac{D}{\bar{a}^3}\,t$$

where

C_o = $(R_o,\ t = 0)$

ρ = density of the solid.

V. STUDIES NOT COMPLETED

At the time of termination of the research contract the following investigations were underway.

A. SINTERING OF GERMANIUM AND ORGANIC COMPOUNDS

These studies were aimed at finding out whether a correlation can be drawn between sintering mechanism and chemical bonding in solids. It was planned to compare the behavior of metal oxides characterized by a large amount of ionic bonding, with solids covalently bonded. Sixteen runs on Ge spheres at 0.72 to 0.84 Tm, where Tm is the melting temperature of Ge in He and/or H_2, failed to produce sintering, except for one run. This was a rather unexpected result. A rather extensive faceting was found to develop on the Ge microspheres. Organic compounds studied involve: anthracene, pyrene, phenanthrene. In the case of anthracene a distillation mechanism responsible for sintering was clearly indicated.

B. SINTERING UNDER REACTIVE ATMOSPHERE

It was found that the effect of the surrounding atmosphere greatly influenced the rate of sintering of platinum miscrospheres. Thus, no thermal sintering of platinum occurred below 1100°C either in oxygen or in helium; sintering did occur readily in pure hydrogen, however, and to a lesser extent

with up to 10% oxygen in the hydrogen. Some typical data are summarized in Table IV.

TABLE IV

SINTERING OF PLATINUM
180-μ Spheres

(1)	$T \leq 800°C$	H_2	No sintering
(2)	$T = 915°C$	He	No sintering
(3)	$T = 915°C$	O_2	No sintering
(4)	$T = 915°C$	H_2	Sintering. Avg "m" in $x^m = kt$ was 13.
(5)	$T = 915°C$	H_2 + 1-5% O_2	Sintering. Avg "m" = 20.

The peculiar effect of hydrogen in bringing about the rapid loss of surface area of finely divided platinum particles has long been known, but no information on the mechanism of the hydrogen on the mass transport process in platinum is available. It is believed that the reported experiments could eventually throw some light on this effect.

VI. CONFERENCE, PUBLICATIONS, AND LIST OF REPORTS

A. CONFERENCES

Results originating from this research were presented at the following conferences:

Symposium on Diffusion and Sintering, University of Notre Dame, June 15-18, 1959.

International Powder Metallurgy Conference, New York, N. Y., June 1960.

Fourth International Symposium on the Reactivity of Solids, Amsterdam, May 29-June 4, 1960.

American Institute of Metallurgical Engineers, Detroit, April 20, 1960.

American Ceramic Society Meeting, Detroit, September 1960.

Gordon Research Conference on Catalysis, New London, N. H., June 1962.

International Conference on Catalytic Technology, Bressanone, Italy, August 1962.

Seminars in various Institutions and Universities.

It is expected that two more publications will be compiled in the future from the results now on hand.

B. PUBLICATIONS

"Sintering Reactions in Zinc Oxide," J. Appl. Phys. 30, 1705 (1959) by V. J. Lee and G. Parravano.

"Chemical Sintering of Berthollide Compounds," in Solid State Reactivity, P. Zwieteriug Editor, Academic Press, 1960, p. 83 by G. Parravano.

"Sintering of Rutile," in Powder Metallurgy, W. Leszywoski Editor, Interscience, 1961, p. 191 by H. M. O'Bryan and G. Parravano.

"Surface Heterogeneity: A Modern Version," Gazz. Chim. Ital., 91, 467 (1961) by G. Parravano.

"Sintering of Zinc Oxide, J. Am. Ceramic Soc., 46, 449, 1963 by L. F. Norris and G. Parravano.

VII. PERSONNEL TRAINED IN THIS PROGRAM

Undergraduate Students

J. P. Palmer
L. F. Norris (till 1961)

Graduate Students

L. F. Norris
G. Lederle
H. M. O'Bryan
H. J. Pietzsak
S. C. Jones

Postdoctorate

L. Manes

BIBLIOGRAPHY

1. V. J. Lee and G. Parravano, Journal of Applied Physics, Vol. 30, p. 17-35, 1959.

2. L. F. Norris and G. Parravano, Journal of the American Ceramic Society, Vol. 46, p. 449, 1963.

3. R. L. Coble, J. Am. Cer. Soc. 41, 55 (1958).

4. H. M. O'Bryan and G. Parravano, "Sintering of Rutile," in Power Metallurgy, W. Leszwoski Editor, Interscience, p. 191, 1961.

5. G. C. Kuczywski, Trans. AIME 185, 169 (1949).

6. C. Herring in "Physics of Powder Metallurgy," Kingston Ed., McGraw-Hill, 1951.

DISTRIBUTION LIST

(One copy unless otherwise noted)

Air Force Office of Scientific
Research
Washington 25, D.C.
Attn: Solid State Sciences Division 3
Attn: Technical Library (SRGL) 2

ASTIA 10
Arlington Hall Station
Arlington 12, Virginia
Attn: TIPCR

Commander 2
Army Rocket & Guided Missile Agency
Redstone Arsenal, Alabama
Attn: ORDXR-OTL

RAND Corporation 2
1700 Main Street
Santa Monica, California

ARDC
Andrews Air Force Base
Washington 25, D.C.
Attn: RDRS

EOAFRD, ARDC
47 Cantersteen
Brussels, Belgium

HQ, USAF
Washington 25, D.C.
Attn: AFDRT

ARL
Building 450
Wright-Patterson Air Force Base
Ohio
Attn: Technical Library

WADD
Wright-Patterson Air Force Base
Ohio
Attn: WWAD

WADD
Materials Central
Wright-Patterson Air Force Base, Ohio
Attn: Metals & Ceramics Lab.
Attn: Physics Lab.
Attn: Materials Information Branch

Institute of Technology Library
MCLI-LIB, Building 125, Area B
Wright-Patterson Air Force Base, Ohio
Attn: AU

ARL
AFRD
Wright-Patterson Air Force Base, Ohio
Attn: Metallurgy
Attn: Solid State Physics

AFOSR
Holloman Air Force Base, New Mexico
Attn: SRLTL

AFCRL
L. G. Hanscom Field, Bedford, Mass.
Attn: CRRELA

AFFTC
Edwards Air Force Base, California
Attn: FTCTL

AEDC
Arnold Air Force Station, Tennessee
Attn: AEOIM

AFSWC
Kirtland Air Force Base, New Mexico
Attn: SWOI

Office of the Chief of Research
and Development
Department of the Army
Washington 25, D.C.
Attn: Scientific Information

DISTRIBUTION LIST (Continued)

Army Research Office
Box CM, Duke Station
Durham, North Carolina
Attn: CRD-AA-IP

Commanding Officer
Ordnance Materials Research Office
Watertown Arsenal
Watertown 72, Massachusetts
Attn: PS&C Div.

Commanding Officer
Watertown Arsenal Laboratories
Watertown 72, Massachusetts
Attn: Technical Reports Section

Commander
Signal Corps Engineering Laboratory
Fort Monmouth, New Jersey
Attn: SIGFM/EL-RPO

Director
U. S. Naval Research Laboratory
Washington 25, D.C.
Attn: Library

Department of the Navy
Office of Naval Research
Washington 25, D.C.
Attn: Code 423
Attn: Code 421

Officer in Charge
Office of Naval Research
Navy No. 100
Fleet Post Office
New York, New York

Commanding Officer
Naval Radiological Defense
Laboratory
San Francisco Naval Shipyard
San Francisco 24, California

Dr. D. F. Bleil
Associate Technical Director for
Research
U. S. Naval Ordnance Laboratory
White Oak, Silver Spring, Maryland

National Aeronautics & Space Agency
1520 H Street, N.W.
Washington 25, D.C.
Attn: Library

Ames Research Center (NASA)
Moffett Field, California
Attn: Technical Library

High Speed Flight Station (NASA)
Edwards Air Force Base, California
Attn: Technical Library

Langley Research Center (NASA)
Langley Air Force Base, Virginia
Attn: Technical Library

Lewis Research Center (NASA)
21000 Brookpark Road
Cleveland 35, Ohio
Attn: Technical Library

Wallops Station (NASA)
Wallops Island, Virginia
Attn: Technical Library

Division of Research
U.S. Atomic Energy Commission
Division Office
Washington 25, D.C.

U.S. Atomic Energy Commission
Library Branch
Technical Information Division, ORE
P. O. Box E
Oak Ridge, Tennessee

DISTRIBUTION LIST (Concluded)

Major John Radcliffe
ANP Office
U.S. Atomic Energy Commission
Washington 25, D.C.

Oak Ridge National Laboratory
P. O. Box P
Oak Ridge, Tennessee
Attn: Central Files

Brookhaven National Laboratory
Upton, Long Island, New York
Attn: Research Laboratory

Argonne National Laboratory
9700 S. Cass Avenue
Argonne, Illinois
Attn: Library

Document Custodian
Los Alamos Scientific Laboratory
P. O. Box 1663
Los Alamos, New Mexico

Ames Laboratory
Iowa State College
P. O. Box 14A, Station A
Ames, Iowa

Knolls Atomic Power Laboratory
P. O. Box 1072
Schenectady, New York
Attn: Document Librarian

National Science Foundation
1901 Constitution Avenue, N.W.
Washington 25, D.C.

National Bureau of Standards Library
Room 203, Northwest Building
Washington 25, D.C.

Director
Office of Technical Services
Department of Commerce
Technical Reports Branch
Washington 25, D.C.

Chairman
Canadian Joint Staff
2450 Massachusetts Avenue, N.W.
Washington, D.C.
Attn: DRB/DSIS

Defense Research Member
Canadian Joint Staff
Director of Engineering Research
Defense Research Board
Ottawa, Canada
Attn: Mr. H. C. Oatway

Institute of the Aeronautical Sciences
2 East 64th Street
New York 21, New York
Attn: Librarian